

Electrocatalysis of Nitric Oxide Reduction by Water-Soluble Cobalt Porphyrin. Spectral and Electrochemical Studies

Shu-Hua Cheng and Y. Oliver Su*

Department of Chemistry, National Taiwan University, Taipei, Taiwan 10764, Republic of China

Received July 20, 1993[⊗]

Water-soluble cobalt tetrakis(*N*-methyl-2-pyridyl)porphine (Co(2-TMPyP)) has been investigated for their catalytic behavior toward nitric oxide reduction. The acid dissociation constants (pK_a) for $[\text{Co}^{\text{III}}(2\text{-TMPyP})(\text{H}_2\text{O})_2]^{5+}$ are 5.5 and 9.6. Nitrite anion coordinates to the Co(III) center in pH 4–12 buffer solutions. The nitrite complex $[\text{Co}^{\text{III}}(2\text{-TMPyP})(\text{NO}_2^-)]^{4+}$ exhibits IR bands at 1401, 1306 and 830 cm^{-1} , indicating a cobalt-nitro complex. The 5-coordinated cobaltous porphyrin, $[\text{Co}^{\text{II}}(2\text{-TMPyP})(\text{H}_2\text{O})]^{4+}$, has been identified by ESR and has $pK_a = 13.0$. This is the first case that the pK_a of a Co(II) porphyrin is presented. Nitric oxide from the disproportionation of nitrite anion in acidic solution can coordinate to the Co(II) center. Resonance Raman spectrum of $[\text{Co}^{\text{II}}(2\text{-TMPyP})(\text{NO})]^{4+}$ exhibits a peak at 1722 cm^{-1} , which disappears upon exposure to air. Electrocatalytic reduction of $[\text{Co}^{\text{II}}(2\text{-TMPyP})(\text{NO})]^{4+}$ at -0.3 V in pH 4.0 buffer solution generates nitrous oxide in a slow rate. Bulk electrolysis was also conducted at -0.7 V , at which $[\text{Co}^{\text{I}}(2\text{-TMPyP})]^{3+}$ reacts with nitrite anion and nitric oxide. The reduction products are mainly ammonia and hydroxylamine.

Introduction

Assimilatory nitrite reductases catalyze the six-electron reduction of nitrite to ammonia.¹ The assimilatory enzymes possess a heme prosthetic group of the isobacteriochlorin type called siroheme, which serves as the binding and active site. The catalytic reduction of nitrite proceeded via the formation of a siroheme–nitrosyl complex, which is then reduced to ammonia. The nitrosyl complex is also observed as the steady-state species during enzyme turnover.² While no other intermediates have been observed in the operating enzyme, hydroxylamine can be reduced by the enzyme, though at a slower rate than nitrite, and is thought to be an intermediate in the reduction. Dissimilatory nitrite reductases reduce nitrite ion to nitrous oxide, nitric oxide, and/or dinitrogen.³ The dissimilatory nitrite reductases contain four hemes, two of *c* and two of *d*₁. The details of the reduction are not known, and it has been the aim of several research groups to characterize intermediates in the reduction and to elucidate the reduction mechanism using model complexes.

Metalloporphyrins and many metal complexes serve many functions in biological systems. Previous work has shown that iron porphyrin nitrosyls, Fe(P)(NO), where P = tetraphenylporphyrin (TPP), tetraphenylchlorin (TPC), or octaethylporphyrin (OEP), are reduced in two one-electron steps in nonaqueous solvents.⁴ The reduction of nitrite to ammonia has been mimicked electrochemically in aqueous solution by utilizing a water-soluble iron porphyrin, Fe(TSPP), (TSPP = dianion of tetrakis(4-sulfonatophenyl)porphyrin).⁵ Metal cyclam com-

plexes, especially the classical 14-membered 1,4,8,11-tetraazacyclotetradecane macrocycle complexes of cobalt and nickel, act as excellent catalysts for the reduction of nitrate and nitrite in aqueous solutions.⁶ At several metal and phthalocyanine-coated electrodes, nitrate and nitrite ions are reduced to mixtures of products that include dinitrogen, hydroxylamine, and ammonia.⁷ Nitrite ion can be reduced to ammonia when bound as a ligand in polypyridyl complexes of Ru(II) or Os(II).⁸ These reactions occur through a series of sequential, stepwise reactions following the initial acid–base conversion of nitrite into nitrosyl.

In this work, we utilize $[\text{Co}(2\text{-TMPyP})]^{5+}$ as an electrocatalyst for the reduction of nitrite in acidic solutions. It was shown that the proximity of the *N*-methylpyridinium group to the porphine ring has strong effects on the axial ligand coordination properties and the redox potential of metalloporphyrins.⁹ The strong electron-withdrawing substituents make the cobalt porphyrin a robust catalyst for NO catalytic reduction. We attempt to uncover pathways for the redox transformations of nitrite ion to ammonia. The approach that has been taken has been (1) to identify the multiple electron transfer reaction (2) to establish the mechanistic details of the individual steps, and, hopefully, (3) the design of models for enzymatic sites that carry out the same or related reactions.

Experimental Section

Cobalt tetrakis(*N*-methyl-2-pyridyl)porphine was synthesized as perchlorate salt according to literature methods.¹⁴ The yield of metalation was 64%. ¹H NMR (in DMSO-*d*₆): δ 3.73–4.23 (m,12H), 8.71–9.35 (m,12H), 9.56–9.59 (m,8H), 9.61–9.77 (m,4H). The multiplicity of resonances is attributed to atropisomerism of this

* Author to whom correspondence should be addressed.

[⊗] Abstract published in *Advance ACS Abstracts*, November 1, 1994.

- (1) (a) Vega, J. M.; Kamin, H. *J. Biol. Chem.* **1977**, *252*, 896. (b) Murphy, M. J.; Siegel, L. M.; Tove, S. R.; Kamin, H. *Proc. Natl. Acad. Sci. U.S.A.* **1974**, *71*, 612. (c) Losada, M. *J. Mol. Catal.* **1975**, *1*, 245.
- (2) (a) Chen, S.-M.; Su, Y. O. *J. Electroanal. Chem.* **1990**, *280*, 189. (b) Younathan, J. N.; Wood, K. S.; Meyer, T. J. *Inorg. Chem.* **1992**, *31*, 3280. (c) Rhodes, M. R.; Barley, M. H.; Meyer, T. J. *Inorg. Chem.* **1991**, *30*, 629.
- (3) (a) Kuwabata, S.; Uezumi, S.; Tanaka, K.; Tanaka, T. *Inorg. Chem.* **1986**, *25*, 3018 and references therein. (b) Henry, Y.; Bessieres. *Biochimie* **1984**, *66*, 259.
- (4) Choi, I.-K.; Liu, Y.; Feng, D.; Paeng, K.-J.; Ryan, M. D. *Inorg. Chem.* **1991**, *30*, 1832.

- (5) Barley, M. H.; Takeuchi, K. J.; Meyer, T. J. *J. Am. Chem. Soc.* **1986**, *108*, 5876.

- (6) Li, H.-L.; Anderson, W. C.; Chambers, J. Q.; Hobbs, D. T. *Inorg. Chem.* **1989**, *28*, 863.

- (7) (a) Li, H.-L.; Robertson, D. H.; Chambers, J. Q.; Hobbs, D. T. *J. Electrochem. Soc.* **1988**, *135*, 1154. (b) Li, H.-L.; Chambers, J. Q.; Hobbs, D. T. *J. Appl. Electrochem.* **1988**, *18*, 454.

- (8) (a) Murphy, W. R., Jr.; Takeuchi, K. J.; Barley, M. H.; Meyer, T. J. *Inorg. Chem.* **1986**, *25*, 1041. (b) Thompson, M. S.; Meyer, T. J. *J. Am. Chem. Soc.* **1981**, *103*, 5577.

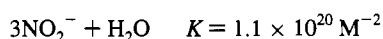
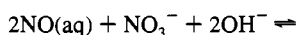
- (9) (a) Su, Y. O. Ph.D. Thesis, The Ohio State University, **1985**. (b) Chan, R. J. H.; Su, Y. O.; Kuwana, T. *Inorg. Chem.* **1985**, *24*, 3777. (c) Ni, C.-L.; Anson, F. C. *Inorg. Chem.* **1985**, *24*, 4754.

porphyrin which arises from restricted rotation about the aryl-porphine bond.²⁷ The porphyrin is diamagnetic and, therefore, that the cobalt ion is in its 3+ oxidation state.²⁸ The IR spectrum (KBr disk) has bands at 3402 (s), 3071 (m), 1616 (s), 1570 (s), 1499 (s), 1447 (w), 1351 (m), 1276 (s), 1139 (vs), 1084 (vs), 1002 (s), 939 (w), 782 (s), 708 (w), 626 (s), and 438 (w) cm^{-1} . Calcd for $\text{Co(2-TMPyP)(ClO}_4)_5 \cdot 6\text{H}_2\text{O}$, $\text{C}_{44}\text{H}_{36}\text{CoN}_8\text{Cl}_5\text{O}_{20} \cdot 6\text{H}_2\text{O}$: C, 39.39; H, 3.58; N, 8.36. Found: C, 39.24; H, 3.24; N, 8.25.

The nitrite coordination compound was prepared by addition of 0.1 M sodium nitrite into 8 mM $[\text{Co(2-TMPyP)}]^{5+}$ aqueous solution. UV-vis spectrum indicates that the species is coordinated with nitrite. Then 0.1 M sodium perchlorate was added and the mixture was stored in refrigerator overnight. The isolated precipitate exhibits new IR bands at 1401, 1306, and 830 cm^{-1} , indicating a nitro complex of Co(III) .²⁹

The nitric oxide-coordinated compound was prepared by bubbling of nitric oxide through a degassed aqueous solution of $[\text{Co}^{\text{III}}(2\text{-TMPyP})]^{5+}$ until the solution exhibited the absorption spectrum of $[\text{Co}^{\text{II}}(2\text{-TMPyP})(\text{NO})]^{4+}$ at 412 and 540 nm. Resonance Raman spectra were obtained via backscattering of sample in a glass tube. The scattered light was focused onto the slit of a spectrometer (Spex Model 1403) equipped with a PMT detector. Excitation were provided by a Krypton ion laser (Coherent Model Innova 400).

Nitric oxide was generated chemically according to¹⁰



Saturated sodium nitrite was added dropwise to 0.2 M H_2SO_4 solution, and the reaction was carried out under nitrogen atmosphere. Nitric oxide was then guided into the cell of interest.

All chemicals are of analytical grade. Aqueous solutions were prepared with doubly distilled deionized water. Buffer solutions were prepared with H_2SO_4 , sodium acetate, phosphate, borate, carbonate and NaOH for pH 0–14. The pH values were measured with a SUNTEX Model 2000 pH meter. Solutions were deoxygenated by purging with prepurified nitrogen gas. Experiments were conducted at room temperature $22 \pm 2^\circ\text{C}$.

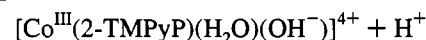
Electrochemistry was performed with a Bioanalytical System Model CV-27 potentiostat and a BAS X-Y recorder. Cyclic voltammetry (CV) was conducted with the use of a three-electrode cell in which a BAS glassy carbon electrode (area = 0.07 cm^2) was used as the working electrode. The glassy carbon electrode (GCE) was polished with 0.05 μm alumina on a Buehler felt pad. The auxiliary compartment contained a platinum wire which was separated by medium-size glass frit. All cell potentials were taken with a Ag/AgCl (saturated KCl) reference electrode. The adsorbed cobalt porphyrin electrode was prepared by immersing the polished GCE in a 1.0 mM $[\text{Co}^{\text{III}}(2\text{-TMPyP})]^{5+}$ solution for 10 min. The electrode was then rinsed with distilled water, and used immediately. OTTLE (optically transparent thin-layer electrode) cell was composed of a 1 mm cuvette, a thin-layer vitreous carbon electrode as a working electrode, and a Ag/AgCl reference electrode. The absorption spectra were obtained with a Hewlett-Packard Model 8452A spectrophotometer. The $^1\text{H-NMR}$ spectra were obtained with a Bruker AM-200WB instrument at 200 MHz using $\text{d}_6\text{-DMSO}$ as solvent. The IR spectra were obtained with a Perkin-Elmer 983 instrument. The elemental analysis was obtained with a Perkin-Elmer 2400 instrument. The ESR spectra were obtained with a Bruker ESP 300 X-band instrument at 77 K. Chemically prepared sample was prepared and sealed under nitrogen atmosphere, then immediately frozen in liquid N_2 . Diphenylpicrylhydrazyl (DPPH) was employed as a $g = 2.00363$ reference material.

Controlled-potential electrolysis of nitrite was carried out in aqueous solutions containing 0.3 M buffer solution at room temperature under nitrogen atmosphere. The electrolysis cell consists of three compartments: one for the vitreous carbon electrode, the second for a platinum counter electrode, which was separated from the vitreous electrode by a medium size frit, and the third for a Ag/AgCl reference electrode. The reduction currents during the electrolysis was recorded with a BAS RYT recorder. The number of electrons consumed in the reduction

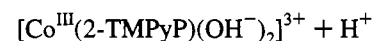
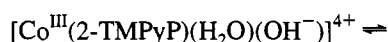
was calculated from the area of the $i-t$ curve. The products from electrocatalysis were determined by the procedures as the following. Ammonia concentration was determined by a SUNTEX Model-3000A ion analyzer. In the process, 3 mL of the electrolysis solution was diluted by a factor of 5, and 0.15 mL of 10 M NaOH was added. The reading was recorded and the ammonia concentration was calculated from a calibration curve. Hydroxylamine concentration was determined by a specific colorimetric test in literature.²⁰ In the process, 0.2 mL of the electrolysis solution, 3 mL of 0.3 M KHP, and 1 mL of 0.01 M ferrozine were mixed and diluted to 8 mL with deionized water. After addition of 2 mL of 0.01 M FeCl_3 , the reaction was allowed to proceed for 7 min and the absorbance was then recorded at 564 nm with the use of a 0.2 cm cuvette. The hydroxylamine concentration was calculated from the calibration curve.

Results and Discussion

A. Spectral and Electrochemical Studies of Co(2-TMPyP) . The absorption spectra of $[\text{Co}^{\text{III}}(2\text{-TMPyP})(\text{H}_2\text{O})_2]^{5+}$ in various pH solutions are paralled to the $[\text{Co}^{\text{III}}(4\text{-TMPyP})(\text{H}_2\text{O})_2]^{5+}$ and $[\text{Co}^{\text{III}}\text{TSP}(\text{H}_2\text{O})_2]^{3-}$ systems.^{11,21} From the spectrophotometric pH titration of $[\text{Co}^{\text{III}}(2\text{-TMPyP})(\text{H}_2\text{O})_2]^{5+}$ in aqueous solution, the absorbance changes correspond to the following equilibrium:



$$\text{p}K_{\text{a}1} = 5.5$$

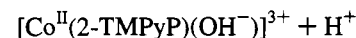


$$\text{p}K_{\text{a}2} = 9.6$$

Owing to the electron-withdrawing ability and the proximity of the *N*-methylpyridinium group to the porphine ring, $[\text{Co}^{\text{III}}(2\text{-TMPyP})(\text{H}_2\text{O})_2]^{5+}$ has smaller $\text{p}K_{\text{a}}$'s than $[\text{Co}^{\text{III}}\text{TSP}(\text{H}_2\text{O})_2]^{3-}$ and $[\text{Co}^{\text{III}}(4\text{-TMPyP})(\text{H}_2\text{O})_2]^{5+}$.

Figure 1A shows the cyclic voltammogram of $[\text{Co}^{\text{III}}(2\text{-TMPyP})]^{5+}$ in pH 4.0 aqueous solution under nitrogen atmosphere. The formal potential (E°) at +0.35 V corresponds to the redox couple of $[\text{Co}^{\text{III/II}}(2\text{-TMPyP})]^{5+/4+}$. The redox potential of $\text{Co}^{\text{III/II}}$ couple is more positive for Co(2-TMPyP) than that of Co(4-TMPyP) by about 0.16 V.⁹ Parallely, the reported redox potential of $[\text{Fe}^{\text{III/II}}(2\text{-TMPyP})]^{5+/4+}$ couple is more positive than that of $[\text{Fe}^{\text{III/II}}(4\text{-TMPyP})]^{5+/4+}$ by about 0.13 V.^{2a} The peak-to-peak separation of $[\text{Co}^{\text{III/II}}(2\text{-TMPyP})]^{5+/4+}$ redox is approximately 140 mV, indicating a slow heterogeneous electron transfer rate.²⁶

The spectra of $[\text{Co}^{\text{II}}(2\text{-TMPyP})(\text{H}_2\text{O})]^{4+}$ obtained from chemical reduction of $[\text{Co}^{\text{III}}(2\text{-TMPyP})]^{5+}$ by sodium ascorbate²³ were consistent with those obtained from OTTLE experiment. The absorbance of $[\text{Co}^{\text{II}}(2\text{-TMPyP})(\text{H}_2\text{O})]^{4+}$ at 416 nm decreased significantly and the peak wavelength red-shifted slightly in more alkaline solutions (pH > 10.7). From the spectral changes, it was proposed that the $\text{p}K_{\text{a}}$ of the ligated H_2O for $[\text{Co}^{\text{II}}(2\text{-TMPyP})(\text{H}_2\text{O})]^{4+}$ is about 13.0 (± 0.2). This is the first case where the $\text{p}K_{\text{a}}$ of a Co(II) porphyrin is presented. The equation is

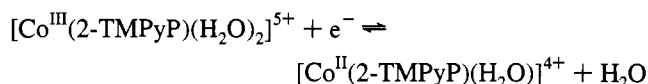


(10) Stanbury, D. M.; DeMaine, M. M.; Doodloe, G. *J. Am. Chem. Soc.* **1989**, *111*, 5496.

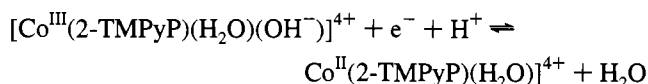
(11) Taniguchi, V. T. Ph.D. Thesis, University of California at Irvine **1978**.

The ESR spectrum of the reduced product of $[\text{Co}^{\text{III}}(2\text{-TMPyP})]^{5+}$ by sodium ascorbate in pH 4.0 buffer solution is characteristic of an axially symmetric spin system assigned as g_{\parallel} and g_{\perp} ($g_{\parallel} = 2.060$, $g_{\perp} = 2.338$ and $A = 105$ G). These regions can further split into an octet by hyperfine splitting (hfs) from the ^{59}Co ($I = 7/2$) nucleus. There is partial resolution of the cobalt hfs in the perpendicular region which is indicative of H_2O , a weak Lewis base, coordinating to the $\text{Co}(\text{II})$ porphyrin.¹³ The reduction product is inferred as a 5-coordinated $[\text{Co}^{\text{II}}(2\text{-TMPyP})(\text{H}_2\text{O})]^{4+}$ according to literature.^{12,13,19}

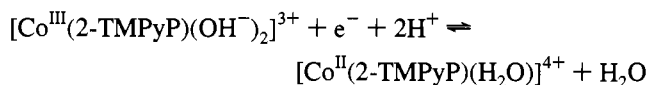
Electrochemical and spectroscopic²² studies of $[\text{Co}^{\text{III}}(2\text{-TMPyP})]^{5+/4+}$ indicate the following redox reactions. At $1.0 < \text{pH} < 5.5$



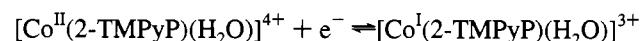
At $5.5 < \text{pH} < 9.6$



At $9.6 < \text{pH} < 13.0$



A reversible redox couple following the $[\text{Co}^{\text{III}}(2\text{-TMPyP})]^{5+/4+}$ coupled was observed at $E^{\circ} = -0.59$ V vs Ag/AgCl . The redox potential is independent of pH at $1.0 < \text{pH} < 14.0$. The reported $[\text{Co}^{\text{III}}(4\text{-TMPyP})]^{5+/4+}$ redox couple occurs at -0.66 V vs. Ag/AgCl in pH 7.4 phosphate buffer.^{9a} Accordingly, the second reversible redox couple is assigned to



The split B band and decrease in intensity are characteristic of $[\text{Co}^{\text{I}}(2\text{-TMPyP})]^{3+}$ and are similar to the reported $[\text{Co}^{\text{I}}(4\text{-TMPyP})]^{3+}$ in DMF¹² and $[\text{Co}^{\text{I}}(\text{TPP})]^-$ in $\text{C}_6\text{H}_5\text{Cl}$.¹⁸ Whether the two-electron reduction product is five- or six-coordinated, is still not known. Table 1 lists the spectral data of $\text{Co}(2\text{-TMPyP})$ at various oxidation states.

B. Nitric Oxide Catalysis by $\text{Co}(2\text{-TMPyP})$. 1. Homogeneous Case. When the solution of $[\text{Co}^{\text{III}}(2\text{-TMPyP})]^{5+}$ in pH 4.0 buffer solution was purged with NO gas, the absorption bands changes from 426, 542, and 574 nm to 412 and 540 nm. The final absorption spectrum was identical with that from $[\text{Co}^{\text{II}}(2\text{-TMPyP})]^{4+}$ purged with NO.^{16,17} Reductive nitrosylation of FeTPPC ^{30a} and MnTPPC ^{30b} have been reported. $[\text{Co}^{\text{II}}(2\text{-TMPyP})(\text{NO})]^{4+}$ is ESR silent in frozen aqueous solution, which is similar to the diamagnetic $\text{Co}^{\text{II}}(\text{OEP})(\text{NO})$ in nonaqueous solution.¹⁵ The nitrosyl complex is stable in oxygen-free solutions. Exposure to air causes the conversion of $[\text{Co}^{\text{II}}(2\text{-TMPyP})(\text{NO})]^{4+}$ to $[\text{Co}^{\text{III}}(2\text{-TMPyP})(\text{NO}_2^-)]^{4+}$ rapidly.

Table 1. Absorption Spectral Data for Various Cobalt Porphyrin Species

	λ , nm ($\epsilon \times 10^{-3}$, $\text{M}^{-1} \text{cm}^{-1}$)	solution
$\text{Co}^{\text{III}}(2\text{-TMPyP})(\text{H}_2\text{O})_2$	426 (212), 542 (21.5), 574 (14.6)	pH 1.0
$\text{Co}^{\text{III}}(2\text{-TMPyP})(\text{H}_2\text{O})(\text{OH}^-)$	426 (133), 542 (18.7), 574 (11.7)	pH 7.5
$\text{Co}^{\text{III}}(2\text{-TMPyP})(\text{OH}^-)_2$	430 (175), 550 (24.7)	pH 13.0
$\text{Co}^{\text{II}}(2\text{-TMPyP})(\text{H}_2\text{O})$	416 (212), 530 (24.7), 560 (22.8)	pH 12.0
$\text{Co}^{\text{I}}(2\text{-TMPyP})(\text{H}_2\text{O})$	418 (74.8), 554 (15.1), 362 (63.4)	pH 12.0
$\text{Co}^{\text{III}}(2\text{-TMPyP})(\text{NO}_2^-)(\text{H}_2\text{O})$	432 (209), 546 (21.8), 570 (10.6)	<i>a</i>
$\text{Co}^{\text{II}}(2\text{-TMPyP})(\text{NO})$	412 (305), 540 (31.3)	<i>a</i>

^a In 0.1 M CH_3COONa , pH 4.0 buffer solution.

$[\text{Co}^{\text{III}}(2\text{-TMPyP})(\text{NO}_2^-)]^{4+}$ rapidly. The resonance Raman spectrum by 415.4 nm excitation of the nitrosyl complex exhibited a new peak at 1722 cm^{-1} . The 1722 cm^{-1} peak disappeared after solution exposure to air. In nitrosyl complexes $\nu(\text{NO})$ ranges from 1500 to 1900 cm^{-1} .²⁹ $\text{Co}^{\text{II}}\text{TPP}(\text{NO})$ was reported to have a $\nu(\text{NO})$ of 1700 cm^{-1} .^{30c} Since the water-soluble porphyrin possesses four strong electron-withdrawing groups, the effect would make the vibration frequency higher. The final product is thus assigned as $[\text{Co}^{\text{II}}(2\text{-TMPyP})(\text{NO})]^{4+}$.

Figure 1B shows the cyclic voltammograms of $[\text{Co}^{\text{II}}(2\text{-TMPyP})(\text{NO})]^{4+}$. The redox couple of $[\text{Co}^{\text{III}}(2\text{-TMPyP})]^{5+/4+}$ is not observed and the irreversible reduction wave at $E_{p,c} = -0.3$ V is considered as the reduction wave of $[\text{Co}^{\text{II}}(2\text{-TMPyP})(\text{NO})]^{4+}$. The reduction currents for this irreversible process (Figure 2B) are compared with those of $[\text{Co}^{\text{III}}(2\text{-TMPyP})]^{5+/4+}$ (Figure 2A) as a function of scan rate. The reduction current is enhanced by doubling in magnitude, indicative of a catalytic reaction. Bulk electrolysis at -0.3 V generates small amount of N_2O as detected by gas chromatography. Small electrolysis current and small quantity of N_2O indicates slow kinetics of the catalytic step.

Another reduction current rose dramatically at about -0.5 V (Figure 1B). The current at -0.6 V is about 10 times as high as that of $\text{Co}^{\text{III}}(2\text{-TMPyP})$ redox couple and is independent of scan rates of $10\text{--}1000$ mV/s. The results suggest that the electron-rich form $[\text{Co}^{\text{I}}(2\text{-TMPyP})]^{3+}$ is more reactive toward NO reduction and the reaction is more complex than reduction by $[\text{Co}^{\text{II}}(2\text{-TMPyP})]^{4+}$. The NO reduction by $[\text{Co}^{\text{II}}(2\text{-TMPyP})]^{4+}$ is a diffusion-controlled step, while the reduction NO by $[\text{Co}^{\text{I}}(2\text{-TMPyP})]^{3+}$ involves multiple steps.

2. Adsorbed Case. Figure 3 shows the cyclic voltammograms of NO reduction catalyzed by adsorbed $\text{Co}(2\text{-TMPyP})$

- (12) Araullo-McAdams, C.; Kadish, K. M. *Inorg. Chem.* **1990**, *29*, 2749.
 (13) Evans, D. F.; Wood, D. J. *Chem. Soc., Dalton Trans.* **1987**, 3099.
 (14) (a) Hambright, P.; Fleischer, E. B. *Inorg. Chem.* **1970**, *9*, 1757. (b) Adler, A. D.; Longo, F. R.; Kampas, F.; Kim, J. J. *Inorg. Nucl. Chem.* **1970**, *32*, 2443. (c) Hambright P.; Gore, T.; Burton, M. *Inorg. Chem.* **1976**, *15*, 2314.
 (15) Fujita, E.; Chang, C. K.; Fajer, J. *J. Am. Chem. Soc.* **1985**, *107*, 7665.
 (16) Hoshino, M.; Arai, S.; Yamaji, M.; Hama, Y. *J. Phys. Chem.* **1986**, *90*, 2109.
 (17) (a) Andrews, M. A.; Chang, T. C.-T.; Cheng, C.-W. F. *Organometallic.* **1985**, *4*, 268. (b) Wayland, B. B.; Minkiewicz, J. V.; Abd-Elmagged, M. E. *J. Am. Chem. Soc.* **1974**, *96*, 2795.
 (18) Dopplet, P.; Fischer, J.; Weiss, R. *Inorg. Chem.* **1984**, *23*, 2958.

- (19) Ozawa, T.; Hanaki, A. *Inorg. Chim. Acta.* **1988**, *153*, 201.
 (20) Dias, F.; Olojola, A. S.; Jaselskis, B. *Talanta* **1979**, *26*, 47.
 (21) Pasternack, R. F.; Cobb, M. A. *J. Inorg. Nucl. Chem.* **1975**, *3*, 599.
 (22) Rohrbach, D. F.; Deutsch, E.; Heineman, W. R.; Pasternack, R. F. *Inorg. Chem.* **1977**, *16*, 2650.
 (23) Martinez, P.; Zuluaga, J. *Inorg. Chim. Acta.* **1988**, *146*, 9.
 (24) Kadish, K. M.; Mu, X. H.; Lin, X. Q. *Inorg. Chem.* **1988**, *27*, 1489.
 (25) Barley, M. H.; Rhodes, M. R.; Meyer, T. J. *Inorg. Chem.* **1987**, *26*, 1746.
 (26) Truxillo, L. A.; Davis, D. G. *Anal. Chem.* **1975**, *47*, 2260.
 (27) (a) Walker, F. A. *Tetrahedron Lett.* **1971**, *52*, 4949. (b) Eaton, S. S.; Eaton, G. R. *J. Am. Chem. Soc.* **1975**, *97*, 3600.
 (28) Pasternack, R. F. *Inorg. Chem.* **1976**, *15*, 643.
 (29) (a) Nakamoto, K. *Infrared and Raman Spectra of Inorganic and Coordination Compounds*, 4th ed.; Wiley: New York, 1986. (b) Ross, S. D. *Inorganic Infrared and Raman Spectra*; McGraw-Hill, London, 1972.
 (30) (a) Wayland, B. B.; Olson, L. W. *J. Am. Chem. Soc.* **1974**, *96*, 6037. (b) Wayland, B. B.; Olson, L. W.; Siddiqui, Z. U. *J. Am. Chem. Soc.* **1976**, *98*, 94. (c) Wayland, B. B.; Minkiewicz, J. V.; Abd-Elmagged, M. E. *J. Am. Chem. Soc.* **1974**, *96*, 2795.

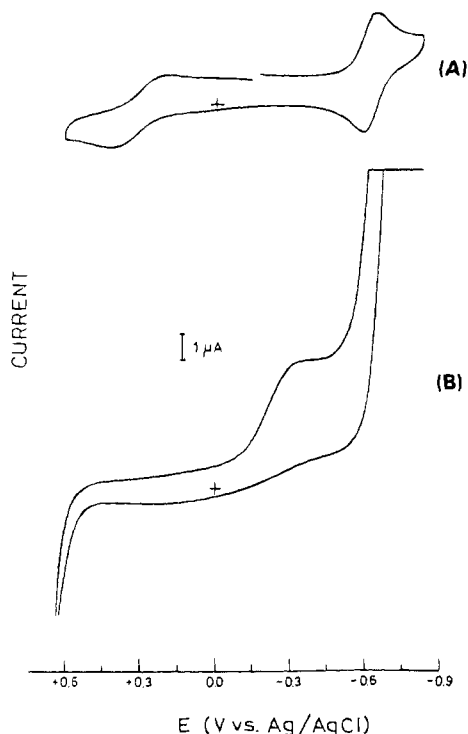


Figure 1. Cyclic voltammogram of 0.31 mM $[\text{Co}^{\text{III}}(2\text{-TMPyP})]^{5+}$ in pH 4.0 sodium acetate buffer solution containing 0.1 M Na_2SO_4 with a scan rate of 0.05 V/s: (A) under N_2 ; (B) under NO.

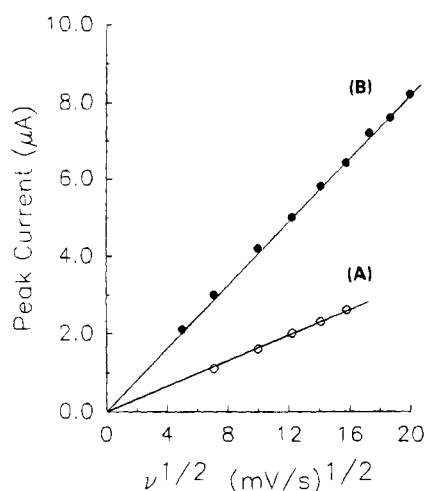


Figure 2. Plot of reduction current vs $v^{1/2}$ for (A) $[\text{Co}^{\text{III}}(2\text{-TMPyP})]^{5+/4+}$ (B) $[\text{Co}^{\text{II}}(2\text{-TMPyP})(\text{NO})]^{4+}$.

and the reduction current rose at about -0.60 V. The catalytic current decreased significantly for each following scan, indicating deactivation of the electrode or desorption of catalyst from the electrode surface. Figure 4 shows the pH dependence of the catalytic current by adsorbed Co(2-TMPyP). The catalytic current decreases as pH increases. The equilibrium concentration of NO depends on the pH value of the solution.¹⁰ So the current decreases for higher pH is probably due to lower NO concentrations in more basic solutions. Another factor is that the reduction mechanism involves proton transfer and hence the pH value also affect the kinetics of the catalytic reaction.

It was reported that cobalt porphyrins were irreversibly adsorbed on carbon electrodes and that their pK_a 's and redox behavior changed.^{9b,9c} The potential dependence vs. pH and oxygen catalysis for adsorbed cobalt porphyrins are different from the solution case. The catalytic current ratio for NO reduction by bulk and adsorbed Co(2-TMPyP) at -0.60 V, the

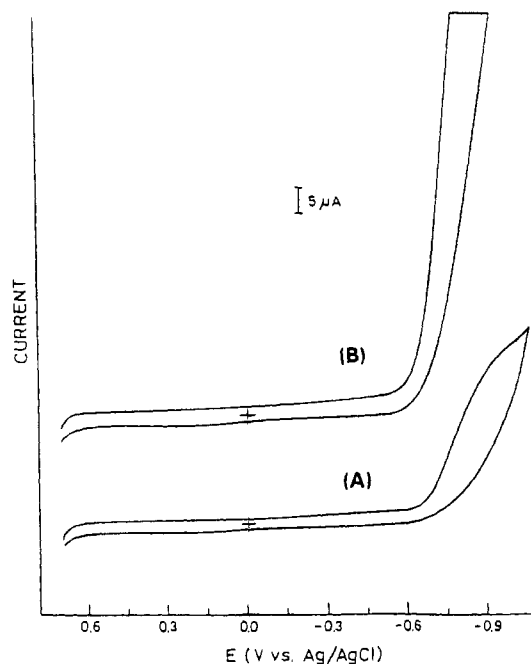


Figure 3. Cyclic voltammogram of NO reduction at (A) a bare glassy carbon electrode or (B) an adsorbed Co(2-TMPyP) electrode in pH 4.0 buffer solution saturated with NO. Scan rate = 0.02 V/s.

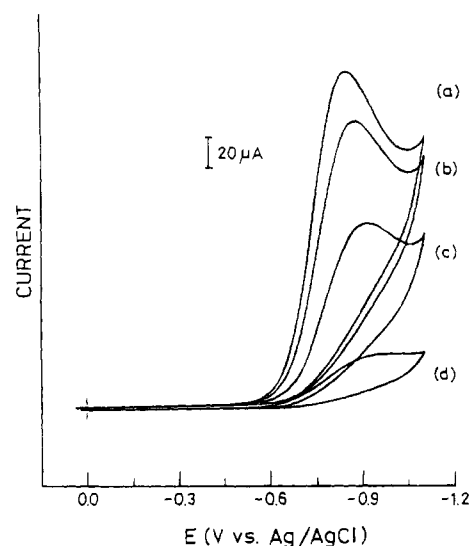


Figure 4. Cyclic voltammogram of NO reduction by adsorbed Co(2-TMPyP) electrode. Scan rate = 0.02 V/s, $[\text{NO}_2^-] = 0.02$ M, pH = (a) 3.46, (b) 4.28, (c) 4.88, (d) 5.87.

$E^{\circ'}$ of the $\text{Co}^{\text{II}}(2\text{-TMPyP})$ couple in the solution, is about 2. The catalytic current has been complicated not only by adsorbed and bulk catalyst but also cobalt porphyrin of different oxidation states. The adsorbed catalysis is probably more efficient in the catalysis since it has thermodynamic and kinetic advantages.³⁴

C. Spectral and Electrochemical Studies of Co(2-TMPyP) in the Presence of Sodium Nitrite. It was shown that $[\text{Co}^{\text{III}}(2\text{-TMPyP})]^{5+}$ is 6-coordinated and weakly bounded with two H_2O ligands in acidic solution. In pH 4.0 buffer solution containing 0.1 M sodium nitrite, the absorption spectrum is red-shifted from 426 to 432 nm, while the absorption in Q band

(31) Suslick, K. S.; Watson, R. A. *Inorg. Chem.* **1991**, *30*, 912.

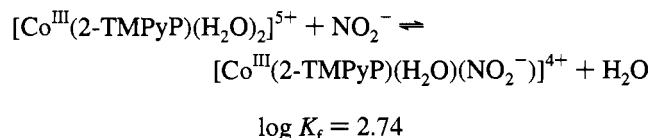
(32) Settin, M. F.; Fanning, J. C. *Inorg. Chem.* **1988**, *27*, 1431.

(33) Tovrog, B. S.; Diamond, S. E.; Mares, F.; Szalkiewicz, A. *J. Am. Chem. Soc.* **1981**, *103*, 3522.

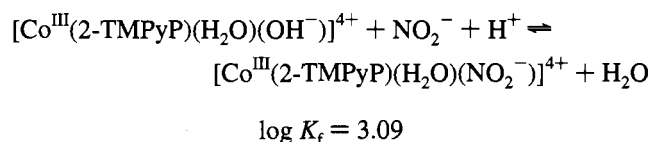
(34) Su, Y.; Kuwana, T.; Chen, S. M. *J. Electroanal. Chem.* **1990**, *288*, 177.

range does not change significantly. In pH 7.0 buffer solution, addition of NaNO_2 to $[\text{Co}^{\text{III}}(2\text{-TMPyP})(\text{H}_2\text{O})(\text{OH}^-)]^{4+}$ resulted in a spectrum identical to that in pH 4.0. The spectral changes obtained upon sodium nitrite addition are assigned as the following reactions.

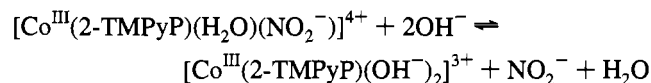
At pH 4.0



At pH 7.0



One of the H_2O ligand of $[\text{Co}^{\text{III}}(2\text{-TMPyP})(\text{H}_2\text{O})_2]^{5+}$ can be replaced by nitrite anion in acidic solution. In neutral and weakly basic solutions, the replacement reaction involves protonation and results in the same product. In more alkaline solution ($\text{pH} > 12.0$), nitrite anion (0.1 M) has no effect on the absorption spectrum of $[\text{Co}^{\text{III}}(2\text{-TMPyP})(\text{OH}^-)]^{3+}$, which indicates that hydroxide is a stronger ligand for Co(III) center and that the ligation ability is about 10 times as strong as that of nitrite anion. The $\text{p}K_a$ value of the H_2O ligated *trans* to NO_2^- could not be obtained by the spectrophotometric titration. The ligated NO_2^- group, on the other hand, can be replaced by the OH^- group in more alkaline solutions ($\text{pH} > 12.0$). The spectral changes are thus assigned to the following reaction:



Some nitrite complexes of metalloporphyrins have been synthesized and characterized.³¹ Manganese porphyrin was coordinated with oxygen-bound nitrite (nitrito form), revealing IR bands at 1444, 1029 and 682 cm^{-1} .³¹ The coordination mode is different from that of the iron³² and the cobalt³³ nitrite complexes, in which the metal centers were nitrogen-bound (nitro form). The nitrite complex of $[\text{Co}^{\text{III}}(2\text{-TMPyP})]^{5+}$ exhibited IR bands at 1401, 1306 and 830 cm^{-1} , which indicated the formation of a cobalt-nitro complex.²⁹

Figure 5 shows the cyclic voltammogram of $[\text{Co}(2\text{-TMPyP})]^{5+}$ in pH 10.0 in the presence of sodium nitrite. The broad peak-to-peak separation of $[\text{Co}^{\text{III/II}}(2\text{-TMPyP})]^{5+/4+}$ couple was improved from 300 to 180 mV in the presence of 19.2 mM NaNO_2 , and the formal potential shifted negatively from +0.04 to -0.09 V. The displacement of nitrite anion upon reduction in pH 10.0 buffer solution was observed by the OTTLE experiment. The absorption peaks at 432, 546 and 570 nm, characteristic of $[\text{Co}^{\text{III}}(2\text{-TMPyP})(\text{H}_2\text{O})(\text{NO}_2^-)]^{4+}$, disappeared at $E_{\text{applied}} = -0.2\text{ V}$ and the absorption peaks at 416, 530 and 560 nm, characteristic of $[\text{Co}^{\text{II}}(2\text{-TMPyP})(\text{H}_2\text{O})]^{4+}$, appeared. The displacement of thiocyanate upon cobalt center reduction had been reported.^{9b}

Figure 6 shows the cyclic voltammogram of $[\text{Co}(2\text{-TMPyP})]^{5+}$ in pH 4.0 in the presence of sodium nitrite. The results were very different from those shown in Figure 5. When 0.4 mM NaNO_2 was added, the reduction current for $[\text{Co}^{\text{III/II}}(2\text{-TMPyP})]^{5+/4+}$ decreased and a new wave appeared at more negative potential. The $[\text{Co}^{\text{III/II}}(2\text{-TMPyP})]^{5+/4+}$ couple disappeared completely and an irreversible wave grew up at -0.3 V

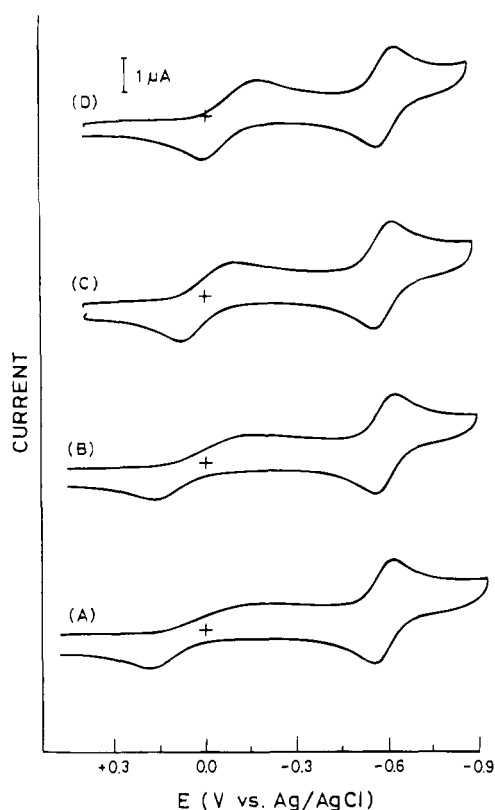


Figure 5. Cyclic voltammograms of $[\text{Co}^{\text{III}}(2\text{-TMPyP})]^{5+}$ in pH 10.0 buffer in the presence of (A) 0, (B) 0.4, (C) 3.2, and (D) $19.2 \times 10^{-3}\text{ M NaNO}_2$. Scan rate = 0.02 V/s.

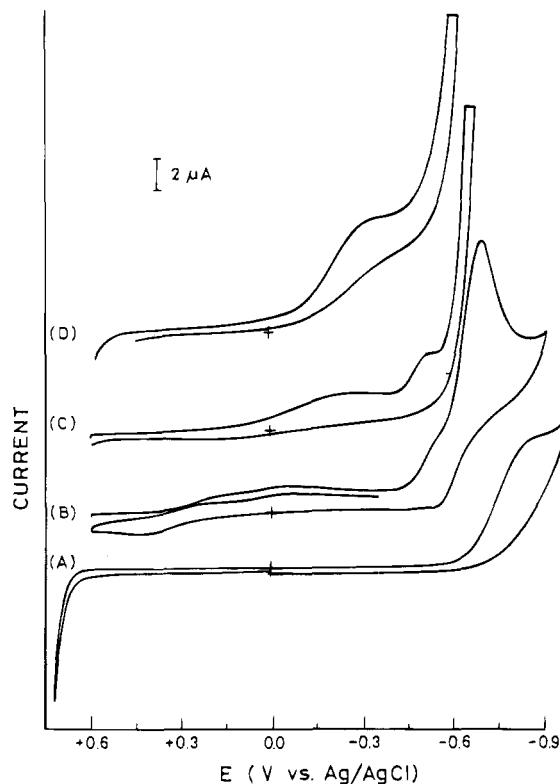


Figure 6. Cyclic voltammograms of (A) 4.4 mM NaNO_2 only, and (B-D) 0.6 mM $[\text{Co}^{\text{III}}(2\text{-TMPyP})]^{5+}$ containing 0.4 (B), 3.2 (C), and $19.2 \times 10^{-3}\text{ M NaNO}_2$ (D), respectively, in pH 4.0 buffer solution. Scan rate = 0.02 V/s.

as the concentration of NaNO_2 increases. The new wave is thus assigned as the reduction of $[\text{Co}^{\text{II}}(2\text{-TMPyP})(\text{NO})]^{4+}$ (Figure 2B, *vide infra*).

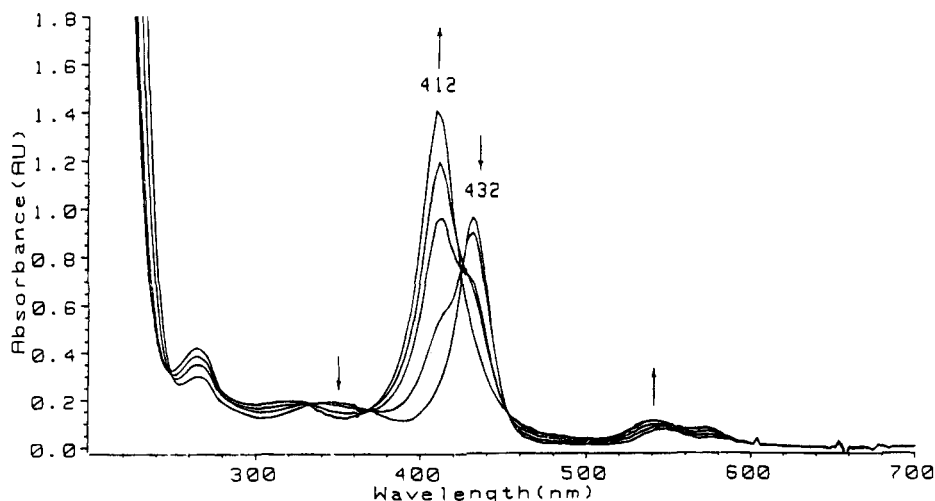


Figure 7. Absorption spectral change of $[\text{Co}^{\text{III}}(2\text{-TMPyP})(\text{H}_2\text{O})(\text{NO}_2^-)]^{4+}$ reduction in pH 4.0 buffer solution. $E_{\text{applied}} = -0.3$ V $[\text{Co}(2\text{-TMPyP}) = 2.3 \times 10^{-4}$ M, $[\text{NO}_2^-] = 0.01$ M.

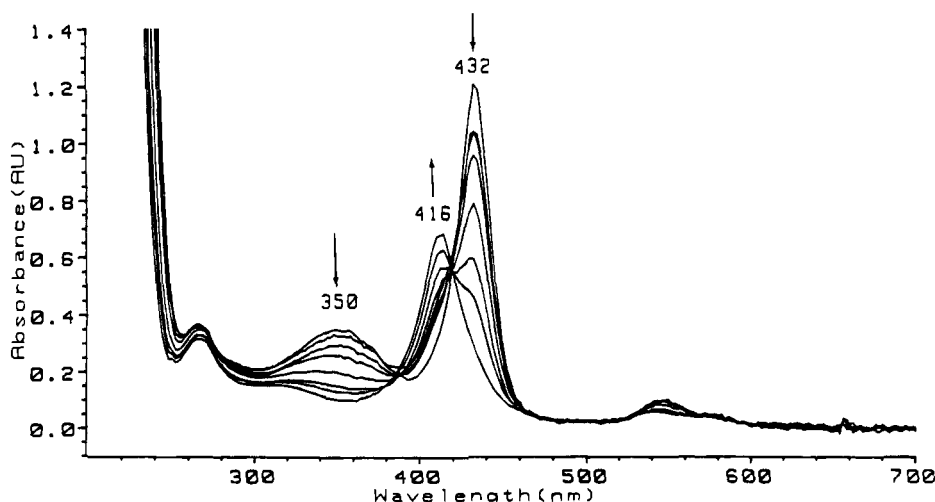
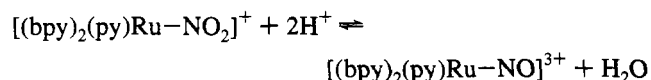


Figure 8. Absorption spectral change of $[\text{Co}^{\text{III}}(2\text{-TMPyP})(\text{H}_2\text{O})(\text{NO}_2^-)]^{4+}$ reduction in pH 4.0 buffer solution. $E_{\text{applied}} = -0.7$ V. Electrolysis time: 78 min. $[\text{Co}^{\text{III}}(2\text{-TMPyP})]^{5+} = 2.8 \times 10^{-4}$ M, $[\text{NO}_2^-] = 0.03$ M.

Figure 7 shows the absorption spectral change for $[\text{Co}^{\text{III}}(2\text{-TMPyP})(\text{H}_2\text{O})(\text{NO}_2^-)]^{4+}$ reduction at -0.3 V in pH 4.0 buffer solution. The resulting spectrum is different from that of $[\text{Co}^{\text{II}}(2\text{-TMPyP})(\text{H}_2\text{O})]^{4+}$. The new peaks at 412 and 540 nm are identical with those of $[\text{Co}^{\text{II}}(2\text{-TMPyP})(\text{NO})]^{4+}$ obtained by direct bubbling NO into $[\text{Co}^{\text{II}}(2\text{-TMPyP})(\text{H}_2\text{O})]^{4+}$ solution. The broad peak at 350 nm, characteristic of nitrite anion, is depleted during $[\text{Co}^{\text{II}}(2\text{-TMPyP})(\text{NO})]^{4+}$ formation and the final spectrum is $[\text{Co}^{\text{II}}(2\text{-TMPyP})(\text{H}_2\text{O})]^{4+}$ after electrolysis for over 24 h. The results indicate that the nitrosyl complex is reduced at -0.3 V and the generated $[\text{Co}^{\text{II}}(2\text{-TMPyP})]^{4+}$ is then ligated by NO from the disproportionation of nitrite in the acidic solution. The catalytic cycle is terminated when nitrite is consumed. The electroreduction reaction in aqueous solution is totally different from that in organic solvent. The reduction of the nitrosyl complex is followed by protonation, as opposed to the loss of NO followed by reaction with CH_2Cl_2 .²⁴

For polypyridyl complex of Ru(II) and Os(II), the nitrosyl complex can be obtained by acid-base conversion between nitrite and the nitrosyl group:⁸



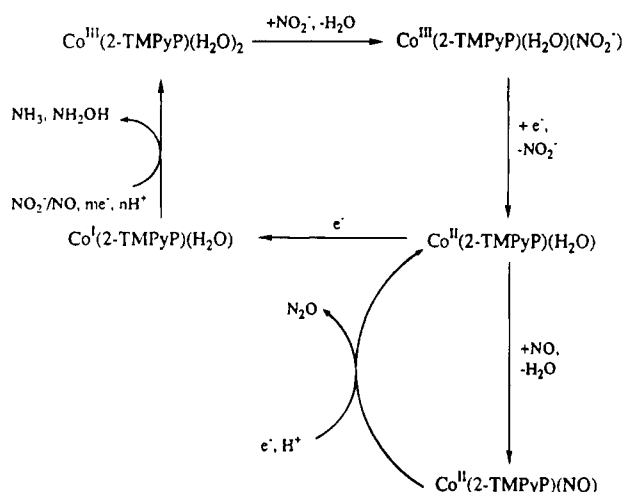
However, in aqueous solution of $[\text{Co}^{\text{III}}(2\text{-TMPyP})]^{5+}$ containing 0.1 M sodium nitrite, $[\text{Co}^{\text{II}}(2\text{-TMPyP})(\text{NO})]^{4+}$ cannot be

obtained by acidification with concentrated sulfuric acid. Therefore, nitrite anion is a strong axial ligand for stabilizing Co(III) center while nitric oxide, an electron deficient ligand, has stronger affinity towards Co(II).

Figure 8 shows the spectral change for the electroreduction of $[\text{Co}^{\text{III}}(2\text{-TMPyP})(\text{H}_2\text{O})(\text{NO}_2^-)]^{4+}$ at -0.7 V in pH 4.0 buffer solution. When the absorption band of nitrite anion at 350 nm is 60% depleted, the B band is still at 432 nm but the intensity decreased by 35%. The nitrite anion is completely consumed after electrolysis for 78 minutes, and B band is then blue-shifted to 418 nm. The final product is $[\text{Co}^{\text{I}}(2\text{-TMPyP})]^{3+}$ and some decomposition of porphyrin appeared. In Figure 5, the nitrite anion has no effect on the potential and shape of the Co^{III} redox wave. However, the absorption spectrum in the electroreduction of $[\text{Co}^{\text{III}}(2\text{-TMPyP})(\text{NO}_2^-)]^{4+}$ containing 0.03 M sodium nitrite at -0.7 V was at 414 nm in pH 10.0 buffer solution, different from that of $[\text{Co}^{\text{I}}(2\text{-TMPyP})]^{3+}$ and indicating interaction between $[\text{Co}^{\text{I}}(2\text{-TMPyP})]^{3+}$ and NO_2^- . The interaction is kinetically slow so that it can not be detected in the time scale of CV measurement. Co^{I} -cyclam was reported to reduce nitrite ion in concentrated NaOH solution.⁶ Therefore, the spectral change in Figure 8 is resulted from the reaction of $[\text{Co}^{\text{I}}(2\text{-TMPyP})]^{3+}$ and NO_2^-/NO .

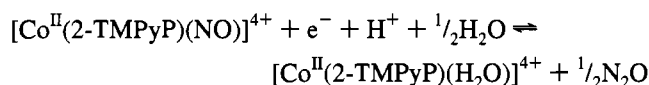
There are some different reactivities between $[\text{Co}^{\text{II}}(2\text{-TMPyP})]^{4+}$ and $[\text{Co}^{\text{I}}(2\text{-TMPyP})]^{3+}$ toward NO_2^-/NO reduction.

Scheme 1



First, $[\text{Co}^{\text{I}}(\text{2-TMPyP})]^{3+}$ catalyzed both NO and NO_2^- reduction, while $[\text{Co}^{\text{II}}(\text{2-TMPyP})]^{4+}$ catalyzed NO reduction only. Secondly, there are kinetic steps for the formation of $[\text{Co}^{\text{II}}(\text{2-TMPyP})(\text{NO})]^{4+}$, while the reduction of $[\text{Co}^{\text{I}}(\text{2-TMPyP})]^{3+}$ toward NO is so rapid that no new spectrum such as $[\text{Co}^{\text{I}}(\text{2-TMPyP})(\text{NO})]^{3+}$ was observed in the time scale of UV/vis measurement.

The electrogenerated $\text{Co}(\text{II})$ and $\text{Co}(\text{I})$ porphyrins catalyzed the nitric oxide reduction to different products is shown in Scheme 1. At -0.3 V, the catalytic center is the cobaltous nitrosyl complex, and gives nitrous oxide. The following reaction is thus proposed:



At more negative potential, $[\text{Co}^{\text{I}}(\text{2-TMPyP})]^{3+}$ catalyzes nitric oxide and nitrite anion reduction to more reduced products, hydroxylamine and ammonia. In the electroreduction of $[\text{Co}^{\text{III}}(\text{2-TMPyP})(\text{H}_2\text{O})_2]^{5+}$ at -0.7 V in pH 4.0 buffer solution containing 2×10^{-3} M NH_2OH , the pattern of spectral changes was identical with that without NH_2OH . Bulk electrolysis of $\text{Co}(\text{2-TMPyP})$ containing NH_2OH in pH 4.0 buffer solution at -0.7 V gave no ammonia. The results indicate that NH_2OH is not an intermediate for NH_3 formation.

D. Products Analysis for the Catalytic Reduction of Nitrite. Controlled-potential electrolysis were carried out and the products analysis are shown in Table 2. The potential was set at -0.7 V for two reasons. First, the catalytic peak potential was about -0.7 V in the cyclic voltammetry. Secondly, the reduction of the pyridinium moiety at -0.9 V is avoided. Cyclic voltammetry at a glassy carbon electrode shows minimal background reduction current for nitrite (Figure 6A).

Figure 9 shows the current-time curves for the bulk electrolysis of 2.0 mM sodium nitrite in pH 4.0 buffer solution. At a bare vitreous carbon electrode, a steady-state current is quickly

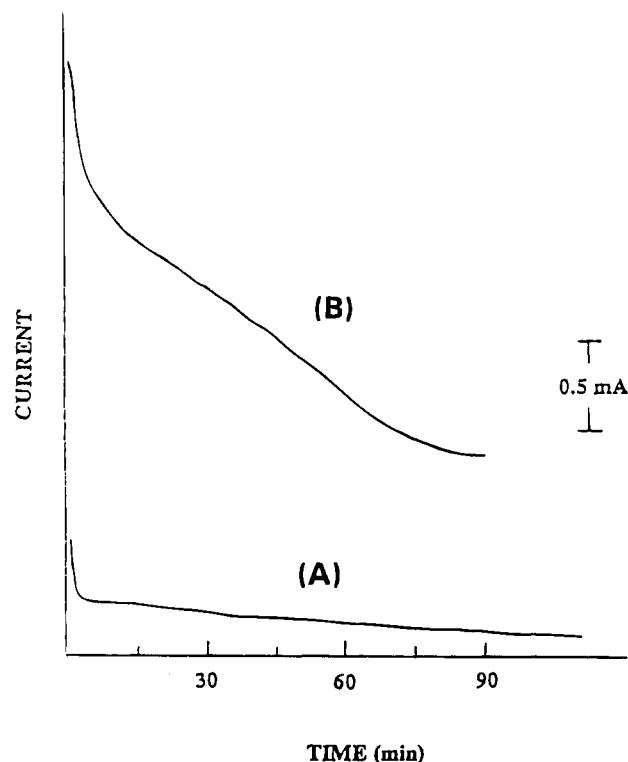


Figure 9. Current–time curves for the bulk electrolysis of 2.0×10^{-3} M sodium nitrite at -0.7 V in pH 4.0 buffer solution (A) without porphyrin catalyst (B) containing 3.1×10^{-5} M $[\text{Co}^{\text{III}}(\text{2-TMPyP})]^{5+}$.

reached and the number of electron transfer is 1.35 per nitrite ion (Figure 9A). Only negligible amount of ammonia and hydroxylamine were obtained from the noncatalyzed reduction. In the presence of 3.1×10^{-5} M $\text{Co}(\text{2-TMPyP})$, the reduction current is over 40 times as much as that without the catalyst. The current decreased gradually with time. The electrolysis was complete when the reduction current fell to 5% of its initial value. The catalytic reduction averagely involves 4.0 electrons per nitrite ion. The products of the catalyzed reduction were mainly hydroxylamine and ammonia.

At pH 4.0, the catalyst was present as the form of $[\text{Co}^{\text{III}}(\text{2-TMPyP})(\text{H}_2\text{O})_2]^{5+}$ before reduction. The absorbance of $[\text{Co}^{\text{III}}(\text{2-TMPyP})]^{5+}$ decreased by 30% after 60 turnovers. The pH value of the solution remained unchanged after electrolysis. The electrolysis at pH 5.0 and 6.0 exhibited lower currents and needed more time for completion. The initial current at pH 6.0 was only a quarter of that at pH 4.0, and the current decreased by 70% after electrolysis for an hour. The product distribution depends on the pH value of the solution.

The reduction current efficiency for the products catalyzed by $\text{Fe}^{\text{III}}(\text{TMPyP})$ was 55% NH_3 , 0% NH_2OH , and 45% N_2O at -0.65 V in pH 4.5 buffer solution. At more negative potential (-0.9 V), the production of N_2O was considerably lower (21% for FeTMPyP and 18% for FeTSP), NH_3 remained significant product (35% and 45%, respectively), and NH_2OH became significant (44% and 37%, respectively).²⁵

Table 2. Products of Electrocatalytic Reductions at $E_{\text{applied}} = -0.7$ V

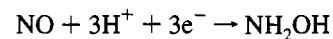
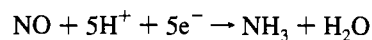
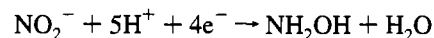
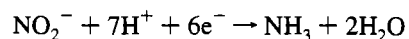
run	$10^5[\text{CoP}]$, mM	$[\text{NO}_2^-]$, mM	$[\text{NO}_2^-]/[\text{CoP}]$	pH	time, min	current mA			n^a	[product], mM	
						i_i	i_f	tot. charge, C		NH_3	NH_2OH
1	3.13	2.0	64	4.0	90	2.5	0.1	4.02	4.16	0.66	1.2
2	3.92	2.0	52	5.0	200	1.1	0.1	4.48	5.02	0.29	1.6
3	3.92	2.0	51	6.0	300	0.7	0.1	3.31	3.43	0.08	0.9
1a	0	2.0		4.0	110	0.6	0.1	1.30	1.35	0.08	0.001

^a Electron added per NO_2^- .

However, there was no N_2O detected by gas chromatography for $[\text{Co}^{\text{III}}(2\text{-TMPyP})]^{+5}$ as summarized in Table 2. Since nitrite is transformed to NH_3 and NH_2OH by nearly 94% at pH 4–5, N_2O formation would be minimal. The ratio of NH_3 is lowered when the solution became more basic (pH > 6). It took more time for complete electrolysis. The results indicate that proton concentration affects NO formation via nitrite disproportionation and thus is involved in the kinetic steps for the electrocatalysis. From the product distribution shown in Table 2, hydroxylamine was always the major product while ammonia was the minor one. The relative ratio of $[\text{NH}_3]/[\text{NH}_2\text{OH}]$ is lower as the pH increases. The electrocatalysis ability of cobalt porphyrin toward nitric oxide reduction was different from that of iron porphyrin, for which hydroxylamine production was minor.

In the electrocatalytic reduction of NO_2^- by water-soluble iron porphyrin, NH_2OH appears to be a precursor of NH_3 . Protonation of NH_2OH hinders coordination and further reduction to NH_3 so that the $\text{NH}_3/\text{NH}_2\text{OH}$ ratio decreases as pH decreases.^{2c} It was reported that cobalt cyclam complex catalyzed sodium nitrite to $\text{NH}_3/\text{NH}_2\text{OH}$ (1/1) in 3.0 M NaOH solution using Hg pool as working electrode.⁶ The $\text{NH}_3/\text{NH}_2\text{-OH}$ ratio decreases as pH increases in the present case may be resulted from the necessity for more protons to reduce both

NO_2^- and NO to NH_3 . On the basis of the stoichiometries of



NH_3 formation requires more protons and is thus less favored in more basic solution.

The activities between CoTMPyP and FeTMPyP monomers for the electrocatalytic oxygen reduction are also different.^{9b,34} Oxygen is transformed to hydrogen peroxide via two-electron reduction by CoTMPyP but to water via totally four-electron reduction by FeTMPyP. The phenomena show that the electrocatalysis ability for cobalt porphyrin toward nitric oxide and oxygen reductions is weaker than that of iron porphyrin. The distinction between iron and cobalt porphyrins is thus worth further study.

Acknowledgment. This work was supported by the National Science Council of the Republic of China.